Small efficient cell-penetrating peptides derived from scorpion toxin maurocalcine.

Cathy Poillot, Hicham Bichraoui, Céline Tisseyre, Eloi Bahemberae, Nicolas Andreotti, Jean-Marc Sabatier, Michel Ronjat, Michel De Waard

Small Efficient Cell Penetrating Peptides Derived From the Scorpion Toxin Maurocalcine*

Cathy Poillot[1,2], Hicham Bichraoui[1,2], Céline Tisseyre[1,2], Eloi Bahemberae[1,2], Nicolas Andreotti[3], Jean-Marc Sabatier[3], Michel Ronjat[1,2] & Michel De Waard[1,2,4]

[1]From Inserm U836, Grenoble Neuroscience Institute, Site santé Tronche, Chemin Fortuné Ferrini, BP170, 38042 Grenoble Cedex 9, France.
[2]Université Joseph Fourier, Grenoble, France.
[3]Inserm UMR1097, Luminy, France ; [4]Smartox Biotechnologies, Floralis, Biopolis, 5 Avenue du Grand Sablon, 38700 La Tronche, France.

Running title: *Small Cell Penetrating Maurocalcine Peptides*

To whom correspondence should be addressed: Dr. Michel De Waard, GIN, Inserm U836, BP170, Grenoble Cedex 09, France. Phone: +(33) 4 56 52 05 63 - Fax: +(33) 4 56 52 06 37 - E-mail: michel.dewaard@ujf-grenoble.fr

Keywords: maurocalcine; cell penetrating peptides; cell delivery; fluorescence

Background: This study aimed at developing a new set of maurocalcine-derived cell penetrating peptides from truncation.
Results: Several truncated peptides were designed and evaluated for Cy5 dye cell penetration.
Conclusion: All truncated peptides are competitive cell penetrating peptides, many of them comparing favorably well to TAT.
Significance: maurocalcine-derived truncated cell penetrating peptides differ in their properties enlarging the potential fields of applications.

SUMMARY

Maurocalcine is the first demonstrated example of an animal toxin peptide with efficient cell penetration properties. While it is a highly competitive cell penetrating peptide (CPP), its relatively large size of 33 amino acids and the presence of three internal disulfide bridges may hamper its development for *in vitro* and *in vivo* applications. Here, we demonstrate that several efficient CPP can be derived from maurocalcine by replacing Cys residues by isosteric 2-aminobutyric acid residues and sequence truncation down to peptides of up to 9 residues in length. A surprising finding is that all the truncated maurocalcine analogues possessed cell penetrating properties indicating that the maurocalcine is a highly specialized CPP. Careful examination of the cell penetrating properties of the truncated analogues indicates that several maurocalcine-derived peptides should be of great interest for cell delivery applications where peptide size matters.

Maurocalcine (MCa) is a 33-mer peptide that was initially isolated from the venom of a Tunisian chactid scorpion, *Scorpio maurus palmatus* (1). The toxin belongs to a family of peptide that folds according to an Inhibitor Cystine Knot (ICK motif), and thus contains three disulfide bridges with a Cys^1-Cys^4, Cys^2-Cys^5 and Cys^3-Cys^6 connecting pattern (2). The solution structure, as defined by ^{1}H-NMR, illustrates that MCa contains three β-strands (strand 1 from amino acid residues 9 to 11, strand 2 from 20 to 23, and strand 3 from 30 to 33). One distinctiveness of MCa is the fact that it is greatly enriched in basic amino acid residues. Out of the 33 amino acids that compose MCa, twelve of them are basic, most of them represented by Lys residues. Interestingly, the β-strands of MCa encompass most of the basic domains (see Fig. 1*A*). MCa turned to be of interest to our research group for several reasons. First, it is an exquisite pharmacological activator of the ryanodine receptor type 1 (RyR1) from skeletal muscle since it promotes high Po gating modes and long-lasting subconductance states of the ion channel (3,4). On myotubes, application of MCa rapidly induces Ca^{2+} release from the sarcoplasmic reticulum (SR) (5), a result further confirmed by positive effect of MCa on the release of Ca^{2+} from purified SR vesicles (3,5). The interaction of MCa

with RyR1 has been witnessed by increased [^{3}H]-ryanodine binding onto purified RyR1 (3,5). The binding site for MCa on RyR1 has also been mapped and shown to correspond to domain(s) that have a predicted localization within the cytoplasm (6). Second, similarly to imperatoxin A (7) for which this was first noted, MCa has an interesting sequence homology with the II-III loop of the L-type calcium channel $Ca_v1.1$ subunit over a domain that is slightly larger than the second β-strand of MCa (see Fig. 1*A*) (5). This loop is predominantly involved in excitation-contraction coupling through direct molecular interactions with RyR1 (6,8). This homology has been a source of inspiration to understand how toxins may interfere with the process of excitation-contraction coupling (4,8,9). Third, and this is the scope of this manuscript, MCa has been shown to act as a cell penetrating peptide (CPP) (10). This discovery stemmed from earlier criticisms that MCa may not be an activator of RyR1 because peptide toxins were not known to cross the plasma membrane, which would be required here to bind to RyR1. Studies that were undertaken to demonstrate the ability of MCa to reach its target showed that i) MCa triggers Ca^{2+} release from the sarcoplasmic reticulum a few seconds after its application in the extracellular medium (5), and ii) intracellular accumulation of fluorescent-streptavidine occurs if it incubated first with biotinylated MCa (10). Since these pioneering studies, MCa or analogues thereof proved powerful vectors for the cell entry of proteins, peptides (11), nanoparticles, or drugs such as doxorubicine (12-15). Although the mode of cell penetration of MCa may vary according to cargo nature, cell type or chemical linkage employed, the data gathered so far suggest that the peptide may enter cells according to two priming steps onto the plasma membrane: first an interaction with proteoglycans with an affinity in the micromolar range, followed by a second interaction with negatively charged lipids which occurs with greater affinity (16,17). The mode of cell entry of MCa is not altered by the absence of proteoglycans, but simply reduced quantitatively, suggesting that proteoglycans do not orient the mode of cell penetration. Two modes seem to concur to MCa cell entry, as far as observed, one related to macropinocytosis and another to membrane translocation. The balance between both modes of entry was found correlated to cargo nature and the type of MCa analogue used.

It is of great interest to pursue the study of MCa as CPP in spite of the wealth of new CPP sequences that are discovered yearly. Among the competitive advantage of MCa over other CPP sequences are the facts that it has almost no associated toxicity *in vitro* and *in vivo*, penetrates into cells at very low concentrations, and is extremely stable *in vivo* upon intravenous injection (over 24 hrs - manuscript in preparation).

While MCa appears as an elaborate and efficient CPP, its pharmacological properties represent a serious hindrance while envisioning *in vitro* and *in vivo* applications. In addition, because of its length (33 amino acid residues) and the presence of three disulfide bridges, MCa is a relatively difficult to synthesize CPP, comparatively to other CPP, and would benefit from a downsizing approach. Several strategies have been successfully employed in the past to overcome one or both of these issues. The first strategy was based on single point mutations of MCa sequence. This strategy preserved the disulfide bridges and the 3D structure of the analogues. Overall, mutations affected more seriously the pharmacology of MCa than the cell penetration properties (18). Many of the amino acids involved in RyR1 binding and pharmacology were located within the cluster of basic amino acids that presented sequence homology with the L-type $Ca_v1.1$ channel. Some of these residues, but not all, were also important for cell penetration properties. Hence, several analogues could be defined that kept close to intact cell penetration properties while entirely losing their pharmacological action (MCa R24A for instance). Some other analogues were actually better than MCa itself for cell penetration suggesting that pairs of mutations, aiming at disrupting pharmacology and improving penetration, may be used in the future to define still better CPP analogues of MCa. The second strategy, that has yield success, is based on the chemical synthesis of D-MCa, an analogue entirely based on the use of D-amino acids. This peptide is a mirror image of the natural L-MCa but, like other D-CPP, preserves its cell penetration properties, while losing entirely its ability to interact with RyR1 (19). This method has several advantages. It no longer is sensitive to proteases which may be an additional advantage for *in vivo* experiments where the half-life of the circulating peptide matters. It is also possible to improve this analogue by introducing point mutations shown previously to improve cell penetration (19). In

these two strategies, while being effective, one may argue that i) the peptides are still among the longest CPP known to date, implying increased costs of production, and ii) the yield of production of these peptides is hampered by the folding process. Also, the use of peptides with internal disulfide bridges, despite have advantageous features in term of stability *in vivo*, makes chemical coupling of these CPP to cargoes more complicated (difficulty to add extra Cys residues to the peptides for instance without interfering with the correct folding process). The third strategy that was used to circumvent one of this criticism was the chemical synthesis of an MCa analogue in which all internal Cys residues where replaced by isosteric 2-aminobutyric acid residues (11). The resulting peptide was still 33-mer long but one step in production was saved by avoiding the folding process. In addition, an extra-Cys residue could be added to the N-terminus of the peptide in order to favor simplified cargo grafting on this CPP analogue. This peptide, termed here C-MCa_{UF1-33} (C for extra-Cys, UF for unfolded, and 1-33 for its length, Fig. 1*B*) has no longer any secondary structures, but efficiently penetrates into cells. Interestingly also, the peptide completely lacks pharmacological activity indicating that folding and secondary structures are essential for binding onto RyR1. While this peptide is an efficient CPP, it remains less potent than MCa in its folded version suggesting that further optimization should be brought to this analogue. Such optimization appears feasible on the basis of the fact that MCa fulfills three different functions (pharmacology, obligation to resemble the L-type channel, and cell penetration). We reasoned that since only cell penetration was the quality we searched for, the peptide could be further simplified and novel analogues be designed.

In this study, we undertook to identify new more potent MCa analogues with three criteria in mind. First, these analogues should be shorter than the folded version of MCa (MCa_F) or the unfolded version (MCa_{UF}). Second, these peptides should be designed in order to better delimitate the domains of MCa responsible for cell penetration. Third, we should be able to design analogues with extra free SH functions for cargo grafting. We present several new analogues that have highly potent cell penetration capabilities, while losing pharmacological activity, preserving lack of cell toxicity, and with facilitated cargo grafting. This new generation of MCa analogues is predicted to have bright futures for CPP applications *in vitro* and *in vivo*.

Experimental procedures

Reagents – N-α-Fmoc-L-aminoacid, Wang-Tentagel resin and reagents used for peptide syntheses were obtained from Iris Biotech. Solvents were analytical grade products from Acros Organics. Cy5 maleimide mono-reactive dye was purchased from GE Healthcare.

Solid-phase peptide syntheses - Chemical syntheses of MCa analogues were performed as previously described (19). Briefly, analogues of MCa were chemically synthesized by the solid-phase method (20) using an automated peptide synthesizer (CEM© Liberty). Peptide chains were assembled stepwise on 0.24 mEq of Fmoc-D-Arg-Pbf-Wang-Tentagel resin using 0.24 mmol of N-α-fluorenylmethyloxycarbonyl (Fmoc) L-amino-acid derivatives. The side-chain protecting groups were: Trityl for Cys and Asn, *tert*-butyl for Ser, Thr, Glu and Asp, Pbf for Arg and *tert*-butylcarbonyl for Lys. Reagents were at the following concentrations: Fmoc-amino-acids (0.2 M Fmoc-AA-OH in dimethylformamide (DMF)), activator (0.5 M 2-(1H-benzotriazole-1-yl)-1,1,3,3-tetramethyluronium hexafluorophosphate in DMF), activator base (2 M diisopropylethylamine in N-methyl-pyrrolidone (NMP)) and deprotecting agent (5% piperazine / 0.1 M 1-hydroxybenzotriazole in DMF), as advised by PepDriver (CEM©). After peptide chain assembly, resins were treated 4 hrs at room temperature with a mixture of trifluoroacetic acid/water/triisopropylsilan (TIS)/dithiothreitol (DTT) (92.5/2.5/2.5/2.5). The peptide mixtures were then filtered and the filtrates were precipitated by adding cold *t*-butylmethyl ether. The crude peptides were pelleted by centrifugation (10.000 × g, 15 min) and the supernatants were discarded. MCa analogues were purified by HPLC using a Vydac C18 column (218TP1010, 25×10 cm). Elutions of the peptides were performed with a 10-60% acetonitrile linear gradient containing 0.1% trifluoroacetic acid. The purified fractions were analyzed by analytical RP-HPLC (Vydac C18 column 218TP104, 25 × 4.6 cm). All analogues were characterized by MALDI-TOF mass spectrometry.

Labeling of peptide with Cy5 - Each peptide was labeled with Cy5 according to the manufacturer's protocol (GE Healthcare). Peptides were dissolved

at 1 mg/ml in 0.1 M Na_2CO_3 buffer, pH 9.3. 300 µl of the solubilized peptides were added to Cy5-maleimide containing tubes. The mixtures were incubated during 2 hrs at room temperature and then purified by HPLC using an analytical Vydac C18 column. Elution of the Cy5-labeled peptides was performed with a 10-60% acetonitrile linear gradient containing 0.1% trifluoroacetic acid. The pure peak fractions were lyophilized and peptides quantified by UV spectrophotometer at 649 nm.

Cell culture - Chinese hamster ovary (CHO) and F98 cell lines (from ATCC) were maintained at 37°C in 5% CO_2 in F-12 nutrient medium (InVitrogen) supplemented with 10% (v/v, CHO) or 2% (v/v, F98) heat-inactivated fetal bovine serum (InVitrogen) and 100 units/ml streptomycin and penicillin (InVitrogen).

MTT assay **-** Cells were seeded into 96-well micro plates at a density of approximately 8×10^4 cells/well. After 2 days of culture, the cells were incubated for 24 hrs at 37°C with MCa analogues at a concentration of 10 µM. Control wells containing cell culture medium alone or with cells, both without peptide addition, were included in each experiment. 0.1% saponin was used as toxic agent for comparison. The cells were then incubated with 3-(4, 5-dimethylthiazol-2-yl)-2, 5-diphenyl-tetrazolium bromide (MTT) for 30 min. Conversion of MTT into purple colored MTT formazan by the living cells indicates the extent of cell viability. The crystals were dissolved with dimethyl sulfoxide (DMSO) and the optical density was measured at 540 nm using a microplate reader (Biotek ELx-800, Mandel Scientific Inc.) for quantification of cell viability. All assays were run in triplicates.

Confocal microscopy - For analysis of the subcellular localization of MCa-Cy5 analogues in living cells, cell cultures were incubated with the fluorescent peptides for 2 hrs, and then washed with phosphate-buffered saline (PBS) alone. The plasma membrane was stained with 5 µg/ml rhodamine-conjugated concanavalin A (Molecular Probes) for 5 min. Cells were washed once more. Live cells were then immediately analyzed by confocal laser scanning microscopy using a Leica TCS-SPE operating system. Rhodamine (580 nm) and Cy5 (670 nm) were sequentially excited and emission fluorescence were collected in z-confocal planes of 10–15 nm steps.

Fluorescence Activated Cell Sorting – CHO cells were incubated with various concentrations of Cy5-labeled peptides in F-12K culture medium without serum at 37°C for 2 hrs. The cells were then washed with PBS to remove excess extracellular peptide and treated with 1 mg/ml trypsin (Invitrogen) for 5 min at 37°C to detach cells from the surface, and centrifuged at 200 *g* before suspension in PBS. For experiments with the macropinocytosis inhibitor, amiloride, CHO cells were initially washed with F-12K and preincubated for 30 min at 37°C with 1 mM amiloride (Sigma). The cells were then incubated for 2 hrs at 37°C with 1 µM of the Cy5-MCa analogues. For all these experimental conditions, flow cytometry analyses were performed with live cells using a Becton Dickinson FACS LSR II flow cytometer (BD Biosciences). Data were obtained and analyzed using FCS express software (De Novo). Live cells were gated by forward/side scattering from a total of 10,000 events.

Preparation of heavy SR vesicles - Heavy SR vesicles were prepared following the method of Kim et al. (21). Protein concentration was measured by the Biuret method.

[^{3}H]-Ryanodine binding assay - Heavy SR vesicles (1 mg/ml) were incubated at 37°C for 2 hrs in an assay buffer composed of 10 nM [^{3}H]-ryanodine, 150 mM KCl, 2 mM EGTA, 2 mM $CaCl_2$ (*p*Ca = 5), and 20 mM MOPS, pH 7.4. Truncated MCa analogues were added prior to the addition of heavy SR vesicles. [^{3}H]-ryanodine bound to heavy SR vesicles was measured by filtration through Whatman GF/B glass filters followed by three washes with 5 ml of ice-cold washing buffer composed of 150 mM NaCl, 20 mM HEPES, pH 7.4. [^{3}H]-ryanodine retained on the filters was measured by liquid scintillation. Non-specific binding was measured in the presence of 80 µM unlabeled ryanodine. The data are presented as mean ± S.E. Each experiment was performed in triplicate.

Statistical analyses - All data are given as mean ± SD for n number of observations, and statistical significance (p) was calculated using Student's t test.

RESULTS

Non folded truncated maurocalcine peptides are efficient CPP

Figure 1A illustrates the primary structure of MCa with its secondary structures (β strands) and its pattern of disulfide bridges. This peptide will be termed MCa_F, for folded (F) MCa. An earlier report has demonstrated that replacing the six internal

cysteine residues of MCa by Abu residues results in a pharmacologically-inert and unfolded (UF) CPP (MCa_{UF1-33}, Fig. 1*B*). This peptide loses its secondary structures (11). Since this project aims at identifying shorter CPP sequences based on MCa_{UF1-33} sequence by the delivery of Cy5 cargo, we first determined where at the N-terminus (C-MCa_{UF1-33}) or C-terminus (MCa_{UF1-33}-C) the cargo could be best grafted after addition of an extra cysteine residue (C) (Fig. 1*B*). As shown, both vector/cargo complexes Cy5-C-MCa_{UF1-33} and MCa_{UF1-33}-C-Cy5 penetrated efficiently within CHO cells, as estimated by confocal microscopy (Fig. 1*C*) or by FACS (Fig. 1*D*). At 3 µM, a slightly better cell penetration was observed with Cy5 localized at the C-terminus of MCa_{UF1-33}, but this difference was not significant. Since chemical syntheses of truncated MCa_{UF1-33} analogues was facilitated by adding the extra cysteine residue at the C-terminus of the sequence rather than at the N-terminus, we kept on working on the basis of MCa_{UF1-33}-C sequence. Nevertheless, these data indicate for the first time that cargo grafting on the CPP MCa_{UF1-33} can be performed likewise at both extremities of the sequence.

Next, we designed a series of truncated MCa_{UF}-C peptides comprising either a C-terminal truncation (3 analogues: MCa_{UF1-20}-C, MCa_{UF1-15}-C and MCa_{UF1-9}-C), a N-terminal truncation (7 analogues: MCa_{UF8-33}-C, $MCa_{UF11-33}$-C, $MCa_{UF14-33}$-C, $MCa_{UF18-33}$-C, $MCa_{UF20-33}$-C, $MCa_{UF22-33}$-C and $MCa_{UF25-33}$-C), and Both N- and C-terminal truncations (2 analogues: MCa_{UF6-25}-C and $MCa_{UF14-25}$-C) (Fig. 2*A*). All of these analogues were then labeled with Cy5 to investigate their cell penetration properties. Every one of these peptides has been designed in such a way that the cargo would be removed from the peptide upon trypsin cleavage. This was useful for the FACS experiments in which the fluorescence associated to the cells is measured after trypsin treatment, thereby potentially removing the cargo from peptides that would eventually be associated to the outer part of the plasma membrane. The net positive charges of the peptides were drastically different, ranging from 0 (MCa_{UF1-15}-C and MCa_{UF1-9}-C) to +8 (MCa_{UF8-33}-C). However, many of the peptides contained a percentage of positively charged residues equal ($MCa_{UF-25-33}$-C) or superior to MCa_F or MCa_{UF1-33} (8 out of twelve analogues). Three analogues had a lower percentage of basic residues than MCa_F (all three C-terminal truncated analogues, MCa_{UF1-20}-C, MCa_{UF1-15}-C and MCa_{UF1-9}-C).

We first evaluated by FACS the fluorescence accumulation within CHO cells that occurred after 2 hrs incubation with 3 µM of positively charged MCa peptides (net charge ≥ +5; Fig. 2*B*). This first study revealed several unexpected findings. First, all of the charged peptides (8 tested) demonstrated CPP properties. These peptides had all the $K^{22}R^{23}R^{24}$ sequence in common, a cluster of basic amino acid residues shown to contribute to the dose-efficacy of cell penetration of MCa_F in an earlier study (18). Interestingly, removing the last 8 C-terminal amino acids of MCa had little impact on the cell penetration properties (if one compares $MCa_{UF14-25}$-C with $MCa_{UF14-33}$-C). Similarly, the removal of the amino acid region His^6-Asn^{13} did not drastically change cell penetration properties (MCa_{UF6-25}-C *versus* $MCa_{UF14-25}$-C). Second, all peptides appeared to behave better than the reference peptide MCa_{UF1-33}-C, suggesting that sequence truncation of MCa_{UF} may represent a potent strategy to define more efficient CPP. Less positively charged peptides were also tested for their ability to penetrate into CHO cells (Fig. 2*C*). No less surprisingly, all peptides showed CPP properties, including two peptides with no net positive charge (MCa_{UF1-9}-C and MCa_{UF1-15}-C). MCa_{UF1-9}-C appeared as a better CPP than MCa_{UF1-15}-C suggesting that the Abu^{10}-Asp^{15} region introduces no competitive advantage and confirming results shown in Fig. 2*B*. This may represent an inhibitory region because of the presence of Glu^{12} and Asp^{15}, two negatively charged residues. The finding that mutation of Glu^{12} to Ala enhances cell penetration of both MCa_F (18) and MCa_{UF} (11) further supports this conclusion. $MCa_{UF25-33}$-C turned out to have also CPP properties, even though this sequence did not confer a competitive advantage to other MCa CPP analogues as shown in Fig. 2*B*. Two additional experiments were conducted to confirm the specificity of these findings. First, a truncated charybdotoxin peptide was synthesized ($ChTx_{UF1-12}$-C) in which the internal Cys residue was replaced by Abu and an additional C-terminal Cys residue added for Cy5 labeling, as for our MCa_{UF} analogues (Supplementary Fig. 1*A*). As shown by confocal microscopy, $ChTx_{UF1-12}$-C was unable to deliver the Cy5 cargo at a higher concentration of 5 µM. Second, we also designed two MCa_{UF} peptides in which, instead of using Abu derivatives, we mutated internal Cys residues by Ala residues. As shown, both $MCa_{UF1-9(Ala)}$-C and $MCa_{UF14-25(Ala)}$-C worked well for Cy5 delivery into CHO cells

demonstrating that Abu residues were not responsible by themselves for the cell penetration properties of the peptides (Supplementary Fig. 1*B,C*). Ala residues were however not fully equivalent to Abu residues as dose-response curve was slightly better for $MCa_{UF14-25(Ala)}$-C than for $MCa_{UF14-25}$-C, further arguing that Abu residues were not central to the cell penetrating properties of truncated MCa_{UF} peptides (Supplementary Fig. 1*D*). The overall message from this first study is that all truncated MCa_{UF} analogues can behave as CPP at the concentration tested. The findings suggest that MCa is a peptide fully specialized to achieve cell penetration including in domains that are not highly charged.

The intracellular distribution of all truncated MCa_{UF} analogues bear resemblance with that of the full length MCa_{UF}

While all truncated derivatives of MCa_{UF1-33} show cell penetration properties according to the FACS analyses, we examined whether there were differences in intracellular distribution among these peptides. This question was investigated by confocal microscopy after 2 hrs of peptide accumulation into CHO cells (Fig. 3). Interestingly, all peptides showed very resembling intracellular distributions, although the degree of accumulated cell fluorescence varied somewhat with peptide sequences. In confirmation of the FACS results, the peptide that appeared to penetrate the least was the full length unfolded MCa, MCa_{UF1-33}-C-Cy5 (Fig. 3*A*). The vast majority of the fluorescence appears in punctuate dots within the cells. In many cases, these dots appear at higher concentrations within one pole of the cell (see labeling of MCa_{UF8-33}-C-Cy5, $MCa_{UF11-33}$-C-Cy5, $MCa_{UF25-33}$-C-Cy5, and MCa_{UF1-9}-C-Cy5 for instance). On various occasions also, all of the peptides tend to present a sub-plasma membrane distribution, forming a rim of smaller circumference than the concanavalin A labeling itself. This sub-plasma membrane rim localization was more evident for CHO cells labeled with $MCa_{UF14-25}$-C-Cy5 as illustrated in Fig. 4*A*. Finally, more rarely, a direct plasma membrane labeling by the peptide-cargo complex was observable (Fig. 4*B*). This type of labeling could be observed with N-terminal truncated vectors exclusively and was most evident for $MCa_{UF22-33}$-C-Cy5. The staining of the plasma membrane was always diffuse in contrast to intracellular staining which was mainly punctuated. Diffuse membrane labeling was also observed for $MCa_{UF25-33}$-C-Cy5 and $MCa_{UF20-33}$-C-Cy5, two peptides that differ from 2 to 3 amino acids of $MCa_{UF22-33}$-C-Cy5. It was difficult to evidence for the other vector/cargo complexes. We propose that this staining coincides with an alteration of the duration of peptide plasma membrane residency for these truncated MCa_{UF} analogues. The lower occurrence of this diffuse staining for the other truncated variants may reflect faster internalization by endocytosis and/or membrane translocation. Globally, these effects reflect cell entry and distribution tendencies that were hard to quantify and they should therefore be interpreted with caution.

In an attempt to better apprehend peptide behavior at the plasma membrane, we quantified the extent of Cy5 / rhodamine staining colocalization. Rhodamine-positive staining was also Cy5-positive for 63% to 86% of the pixels (best performing peptides were $MCa_{UF14-33}$-C-Cy5, $MCa_{UF18-33}$-C-Cy5, $MCa_{UF20-33}$-C-Cy5 and $MCa_{UF22-33}$-C-Cy5; data not shown). This finding indicates that the peptides invade large membrane areas and that membrane interaction is not limited to small specialized surface areas. In contrast, Cy5-positive pixels were rhodamine-positive to far more variable extents (Fig. 4*C*). For instance, 10.1 ± 2.6% of MCa_{UF1-33}-C-Cy5, the reference compound, was colocalized with the plasma membrane indicator. In spite of the fact that short plasma membrane staining times were used (few minutes), a fraction of the colocalization that is quantified also corresponds to intracellular staining following ongoing endocytosis. Nevertheless, this result indicates that this peptide does not remain stuck within the plasma membrane during its 2 hrs incubation with CHO cells. It indicates relatively fast cell penetration thus. Many of the other peptides however behaved differently from MCa_{UF1-33}-C-Cy5. Indeed, several peptides show surprisingly higher colocalization with rhodamine (21.3 ± 2.6% for $MCa_{UF11-33}$-C-Cy5 and 30.4 ± 1.4% for MCa_{UF1-20}-C-Cy5 for instance). These higher values of colocalization indicate that some peptides remain for longer periods of time or at higher concentration within the plasma membrane. Alternatively, these peptides may rely more heavily on endocytosis for cell penetration and are present within intracellular organelles to which subsequent endocytotic vesicles that contain rhodamine labeling will fuse. Peptides most concerned by these behaviors were $MCa_{UF11-33}$-C-Cy5 and $MCa_{UF14-33}$-C-Cy5, that contained two or one of the CPP inhibitory negative charges

(Glu[12] and Asp[15]), and MCa_{UF1-9}-C-Cy5 and MCa_{UF1-20}-C-Cy5, that were poorly charged peptides.

Amiloride-sensitivity of the cell penetration of truncated MCa_{UF} analogues

In earlier studies, we have demonstrated that the cell entry of MCa_{UF1-33} was largely sensitive to amiloride. Since amiloride is an exquisite blocker of macropinosomes (22-24), this suggested a predominant macropinocytosis mechanism for its cell penetration (17). However, it was likely that such a predominant reliance on macropinocytosis was also conferred by the cargo type transported (streptavidine in that report). We therefore conducted an in depth analysis of the amiloride-sensitivity of the various truncated MCa_{UF} peptides with Cy5 as cargo and quantified by FACS the degree of cell penetration inhibition. Fig. 5*A* illustrates the amiloride-sensitivity of four different truncated peptides. As shown, amiloride inhibits the cell penetration of MCa_{UF1-33}-C-Cy5 by 19.6% and of MCa_{UF1-15}-C-Cy5 by 39%. The finding that amiloride blocks to a far lesser extend the penetration of Cy5 compared to that of streptavidin (17) when MCa_{UF1-33} is the vector indicates the influence of the cargo nature on the mechanism of cell entry. Surprisingly, amiloride was found to enhance rather than inhibit the cell penetration of $MCa_{UF20-33}$-C-Cy5 and $MCa_{UF18-33}$-C-Cy5 (Fig. 5*A*). Preserving the plasma membrane from undergoing macropinocytosis may free surface areas for enhanced peptide translocation through the membrane. The effect of amiloride was always associated with a sharpening of the fluorescence intensity distribution in the x axis (see for instance MCa_{UF1-15}-C-Cy5), reflecting reduced cell heterogeneity for the mechanisms underlying peptide penetration. The amiloride-sensitivity of cell penetration was further investigated for all truncated MCa_{UF} peptides and the results presented in Fig. 5*B*. Four peptides showed higher amiloride-sensitivity than MCa_{UF1-33}-C-Cy5 ($MCa_{UF11-33}$-C-Cy5, $MCa_{UF25-33}$-C-Cy5, MCa_{UF1-15}-C-Cy5 and $MCa_{UF14-25}$-C-Cy5). All other peptides showed reduced amiloride-sensitivities or a tendency for greater cell penetration under the effect of amiloride. We conclude that the Cy5 cargo does not promote macropinocytosis as the main route of peptide entry, and that truncation of MCa_{UF} may lead to analogues that rely to a lesser extent on macropinocytosis for cell entry.

Comparative dose-dependent cell penetration of the MCa_{UF} analogues

While we compared the properties of cell penetration of truncated peptides at rather mild concentrations, we also aimed at comparing the dose-dependence of cell penetration of these peptides by FACS (Fig. 6). One example of such an analysis is shown for peptide MCa_{UF8-33}-C-Cy5 in Fig. 6*A*. 33 µM was the highest concentration that could be tested on CHO cells and obviously cell penetration did not show any sign of saturation for cell incubation times with this peptide of 2 hrs. The dose-dependent cell penetration were compared for all N-terminal truncated peptides (Fig. 6*B*), C-terminal truncated peptides (Fig. 6*C*), and double truncated analogues (Fig. 6*D*) with the same settings. These analyses confirm that MCa_{UF1-33}-C-Cy5 is the least-performing cell penetrating peptide. Most truncated peptides show detectable cell penetration at concentrations equal or above 1 µM. One remarkable exception to this rule was noticeable. MCa_{UF1-9}-C-Cy5 shows an unusual dose-dependent penetration with detectable cell penetration at 10 nM and only small progressive increases in fluorescence intensity with higher peptide concentrations (Fig. 6*C*). This peptide was therefore the best performing peptide for cell penetration at low concentrations. Finally, additional information that could be taken from these analyses is that the peptides differed significantly with regard to the maximal extent of cell penetration. Among the N-terminal truncated MCa_{UF} analogues, $MCa_{UF18-33}$-C-Cy5 performed drastically better than the other truncated peptides (Fig. 6*B*). The difference in cell penetration among $MCa_{UF11-33}$-C-Cy5 and $MCa_{UF18-33}$-C-Cy5 resides in the removal of KENKDAbuAbu sequence which we presume is inhibitory to some extent because of the presence of Glu[12] and Asp[15]. Among the C-terminal truncated peptides, MCa_{UF1-20}-C-Cy5 was performing as well as MCa_{UF8-33}-C-Cy5, and although not tested at higher concentrations, MCa_{UF1-9}-C-Cy5 would be expected to perform still better. Finally, for N- and C-terminal truncated analogues, the best peptide turns out to be $MCa_{UF14-25}$-C-Cy5 that yields the greatest fluorescence accumulation at 33 µM compared to all other truncated MCa_{UF} analogues. While all these peptides performed quite well, we were curious to compare them to a classical CPP under similar experimental conditions. Cell penetration was observed for TAT-C in CHO cells and dose-response curve was equivalent or even less favorable for TAT than for many MCa_{UF} peptides (Supplementary Fig. 1*E,F*). This was

further largely confirmed when comparing the vector properties of TAT-C and MCa_{UF1-9}-C in yet another cell type, the glioma F98 rat cell line (Supplementary Fig. 2). 3 µM MCa_{UF1-9}-C proved better than TAT-C at 3 and 10 µM.

Truncated MCa_{UF} peptides lack pharmacological effects and are predominantly non toxic

An earlier report has shown that MCa_{UF1-33} is unable to interact with MCa's target, the ryanodine receptor RyR1 (11). This is due to the loss of secondary structures owing to the lack of internal disulfide bridging. We did therefore expect that truncated analogues of MCa_{UF} should also be pharmacologically inert. This hypothesis was challenged by testing the ability of the Cy5-free peptides to stimulate [^{3}H]-ryanodine binding (Fig. 7*A*). As shown, contrary to MCa_F that contains secondary structures and disulfide bridges, none of the peptides we designed had an effect on [^{3}H]-ryanodine binding.

Finally, the peptides were challenged for their toxicity by incubating CHO cells with 1 or 10 µM peptide concentrations for an extended duration (24 hrs) that far exceeds the duration challenged for cell penetration (Fig. 7*B*). A 10 µM peptide concentration was generally slightly more toxic than 1 µM, except for $MCa_{UF14-25}$-C. At 1 µM, toxicity never exceeded 8% and significances of these effects were negligible. In contrast, toxicity could reach 20% at 10 µM peptide concentration and these effects had higher significance. Most peptides behaved equally well or better than MCa_{UF1-33}-C indicating that truncation did not enhance cell toxicity of the peptides.

Discussion

MCa_F is a rather large and complex CPP with its three disulfide bridges which makes its use in *in vitro* and *in vivo* applications more delicate because of production yield (peptide with correct disulfide bridging) and cargo coupling (thiol groups are for the moment difficult to use). One may also argue that the size of the peptide introduces additional synthesis cost compared to other popular in use CPP such as Tat and penetratin. While size and folding most likely adds a competitive advantage for *in vivo* applications because of peptide stability issues, it may be of interest to derive small CPP from MCa that could have a broader use than MCa itself. The study we conducted not only aimed at defining these smaller MCa-derived CPP sequences, but also provided interesting clues on how MCa may have evolved for cell penetration. The most surprising finding from this study was therefore that all of the analogues we defined could be considered as CPP, which suggests that MCa is a highly specialized sequence for the purpose of cell penetration. While evidently none of the peptides could compete with MCa_F itself for cell penetration, it is nevertheless obvious that many of the truncated MCa_{UF} peptides are better CPP than MCa_{UF1-33} itself. These findings lead to two general conclusions. First, folding and disulfide bridging appears to be a prerequisite to properly optimize the CPP potential of all the MCa domains. It is highly likely that the secondary structures triggered by disulfide bridging play a key role in that respect. We therefore believe that it would be worthwhile to design additional MCa analogues presenting both truncations (like in the present study) and 1 to 2 disulfide bridges in order to regain some of the secondary structures that confer a competitive advantage to MCa_F for cell penetration. Second, the fact that all the truncated sequences are CPP that possess different properties and efficacies, suggests that there is further room for MCa cell penetrating optimization. In this study, our data indicate that the amino acid region Lys^{11}-Ser^{18} would be an ideal target for mutagenesis. Glu^{12} mutation has already been shown to improve cell penetration on various analogues (11,18). We now sense that Asp^{15} may also represent an excellent target for further optimization of MCa's properties. Double mutagenesis may be an option. However, it will be essential to determine whether the disulfide bridging and folding ability of the native peptide is not affected by this procedure. Truncated MCa_{UF} peptides may also benefit from further mutagenesis of negatively charged residues, such as MCa_{UF1-20}. It is noteworthy that another well behaving truncated CPP, $MCa_{UF18-33}$, also contains a Glu residue at position 29 that could represent another target for mutagenesis and peptide optimization. This is also the case for MCa_{UF1-9} that contains an Asp residue at position 2.

Several other findings of this report merit some comments. First, we demonstrate that cargo coupling can occur at the N-terminus as well as the C-terminus of MCa enhancing the flexibility of cargo coupling to our vectors. Second, while it is obvious that most of our truncated MCa_{UF} analogues remain heavily basic, we also found out that poorly charged MCa peptides could behave as

efficient CPP. This is the case for MCa_{UF1-9} which is one of our best performing CPP, especially if one wishes to work with low CPP concentrations. Third, small size CPP can be derived from MCa_{UF}, MCa_{UF1-9} and $MCa_{UF25-33}$ being our smallest peptides. While we did not test greater truncation, it is not impossible that still smaller CPP might be designed on the basis of MCa sequence. Fourth, the truncated MCa_{UF} analogues differ somewhat in their mode of cell penetration, some being more prone to enter cells by macropinocytosis than others. Various peptides were even insensitive to amiloride application suggesting that macropinocytosis did not contribute at all to their entry. We can't exclude at this stage that these peptides rely on other modes of endocytosis than macropinocytosis. This is suggested by the punctuate nature of intracellular Cy5 fluorescence distribution. How reliably a punctuate distribution reveals endocytosis is however not known, and one can't rule out also that this distribution is due to peptide aggregation with or without lipid components. When plasma membrane distribution could be observed, large diffuse staining was evident indicating that when peptides encountered the membrane no such aggregation occurred. In any case, many of the peptides had distribution that mostly differed from plasma membrane labeling (including these membranes that had undergone endocytosis) indicating that peptide intracellular distribution may not necessarily colocalize with the plasma membrane components. Refined studies will be required however to define how much of the peptides enter cells by direct membrane translocation *versus* endocytosis.

To conclude on this study, we identified several interesting lead CPP based on MCa_{UF} truncation strategy. This is the case for $MCa_{UF18-33}$ (macropinocytosis entry-independent), MCa_{UF1-9} (penetrates better at low concentration), and $MCa_{UF14-25}$ (yields the greatest cell entry of the dye). These peptides are easy to produce, yield good cell penetration, and we should be able to further improve their cell penetrating characteristics by mutagenesis or by reintroducing one disulfide bridge to restore some of the secondary structures. While the scope of this study was not to compare our mini MCa with other popular CPP, we were surprised to find out that many of the MCa_{UF} vectors behaved far better than TAT for the transport of Cy5, both in CHO and F98 cells. It may be argued that the field doesn't require many more CPP sequences. However, a significant fraction of the ongoing research is based on the use of TAT, which no longer appears as the most competitive peptide. Also, increasing evidences suggest that CPP sequences differ in their cell-type targeting properties, which will undoubtedly represent an important feature to exploit when it comes to developing *in vivo* applications. Other essential parameters for in vivo applications will be the peptide stability upon intravenous or intra-peritoneal injection. In that respect, we found out that MCa is a particularly stable peptide with and without disulfide bridges (unpublished observations). These still "hidden" aspects of the CPP features may be advantageously exploited later on if the number of known CPP is high. The advantages of using smaller CPP over MCa_{F} remains to be investigated as one may of course argue also that they require higher concentrations and possibly longer incubation times for effectiveness, two factors that may lead to spurious signaling events *in vivo*.

References

1. Fajloun, Z., Kharrat, R., Chen, L., Lecomte, C., Di Luccio, E., Bichet, D., El Ayeb, M., Rochat, H., Allen, P. D., Pessah, I. N., De Waard, M., and Sabatier, J. M. (2000) *FEBS Lett* **469**, 179-185
2. Mosbah, A., Kharrat, R., Fajloun, Z., Renisio, J. G., Blanc, E., Sabatier, J. M., El Ayeb, M., and Darbon, H. (2000) *Proteins* **40**, 436-442
3. Chen, L., Esteve, E., Sabatier, J. M., Ronjat, M., De Waard, M., Allen, P. D., and Pessah, I. N. (2003) *J Biol Chem* **278**, 16095-16106
4. Lukacs, B., Sztretye, M., Almassy, J., Sarkozi, S., Dienes, B., Mabrouk, K., Simut, C., Szabo, L., Szentesi, P., De Waard, M., Ronjat, M., Jona, I., and Csernoch, L. (2008) *Biophys J* **95**, 3497-3509
5. Esteve, E., Smida-Rezgui, S., Sarkozi, S., Szegedi, C., Regaya, I., Chen, L., Altafaj, X., Rochat, H., Allen, P., Pessah, I. N., Marty, I., Sabatier, J. M., Jona, I., De Waard, M., and Ronjat, M. (2003) *J Biol Chem* **278**, 37822-37831

6. Altafaj, X., Cheng, W., Esteve, E., Urbani, J., Grunwald, D., Sabatier, J. M., Coronado, R., De Waard, M., and Ronjat, M. (2005) *J Biol Chem* **280**, 4013-4016
7. Gurrola, G. B., Arevalo, C., Sreekumar, R., Lokuta, A. J., Walker, J. W., and Valdivia, H. H. (1999) *J Biol Chem* **274**, 7879-7886
8. Szappanos, H., Smida-Rezgui, S., Cseri, J., Simut, C., Sabatier, J. M., De Waard, M., Kovacs, L., Csernoch, L., and Ronjat, M. (2005) *J Physiol* **565**, 843-853
9. Pouvreau, S., Csernoch, L., Allard, B., Sabatier, J. M., De Waard, M., Ronjat, M., and Jacquemond, V. (2006) *Biophys J* **91**, 2206-2215
10. Esteve, E., Mabrouk, K., Dupuis, A., Smida-Rezgui, S., Altafaj, X., Grunwald, D., Platel, J. C., Andreotti, N., Marty, I., Sabatier, J. M., Ronjat, M., and De Waard, M. (2005) *J Biol Chem* **280**, 12833-12839
11. Ram, N., Weiss, N., Texier-Nogues, I., Aroui, S., Andreotti, N., Pirollet, F., Ronjat, M., Sabatier, J. M., Darbon, H., Jacquemond, V., and De Waard, M. (2008) *J Biol Chem* **283**, 27048-27056
12. Aroui, S., Brahim, S., De Waard, M., Breard, J., and Kenani, A. (2009) *Cancer Lett* **285**, 28-38
13. Aroui, S., Brahim, S., Hamelin, J., De Waard, M., Breard, J., and Kenani, A. (2009) *Apoptosis* **14**, 1352-1365
14. Aroui, S., Brahim, S., De Waard, M., and Kenani, A. (2010) *Biochem Biophys Res Commun* **391**, 419-425
15. Aroui, S., Ram, N., Appaix, F., Ronjat, M., Kenani, A., Pirollet, F., and De Waard, M. (2009) *Pharm Res* **26**, 836-845
16. Boisseau, S., Mabrouk, K., Ram, N., Garmy, N., Collin, V., Tadmouri, A., Mikati, M., Sabatier, J. M., Ronjat, M., Fantini, J., and De Waard, M. (2006) *Biochim Biophys Acta* **1758**, 308-319
17. Ram, N., Aroui, S., Jaumain, E., Bichraoui, H., Mabrouk, K., Ronjat, M., Lortat-Jacob, H., and De Waard, M. (2008) *J Biol Chem* **283**, 24274-24284
18. Mabrouk, K., Ram, N., Boisseau, S., Strappazzon, F., Rehaim, A., Sadoul, R., Darbon, H., Ronjat, M., and De Waard, M. (2007) *Biochim Biophys Acta* **1768**, 2528-2540
19. Poillot, C., Dridi, K., Bichraoui, H., Pecher, J., Alphonse, S., Douzi, B., Ronjat, M., Darbon, H., and De Waard, M. (2010) *J Biol Chem* **285**, 34168-34180
20. Merrifield, R. B. (1969) *Adv Enzymol Relat Areas Mol Biol* **32**, 221-296
21. Kim, D. H., Ohnishi, S. T., and Ikemoto, N. (1983) *J Biol Chem* **258**, 9662-9668
22. West, M. A., Bretscher, M. S., and Watts, C. (1989) *J Cell Biol* **109**, 2731-2739
23. Veithen, A., Cupers, P., Baudhuin, P., and Courtoy, P. J. (1996) *J Cell Sci* **109 (Pt 8)**, 2005-2012
24. Meier, O., Boucke, K., Hammer, S. V., Keller, S., Stidwill, R. P., Hemmi, S., and Greber, U. F. (2002) *J Cell Biol* **158**, 1119-1131

FOOTNOTES

This work was supported by grants from Technology pour la Santé (Program TIMOMA2 of the Commissariat à l'Energie Atomique) and from Agence Nationale pour la Recherche PNANO (Programs SYNERGIE and NanoFret). Mass spectrometry analyses were performed by the Centre d'Investigation Clinique of Grenoble under the heading of Dr. Michel Sève.

The abbreviations used are: CD: Circular Dichroism; CPP: Cell Penetrating Peptide; DMF: dimethyformamide; FACS: Fluorescence-Activated Cell Sorting; HPLC: high-performance liquid chromatography; MCa: Maurocalcine; NMP: N-methyl-pyrrolidone; RS: Sarcoplasmic reticulum; RyR: Ryanodine Receptor; TFA: trifluoroacetic acid.

FIGURE LEGENDS

Fig. 1. Efficacy of cargo penetration as a function of grafting position on MCa_{UF1-33}. (A) Amino acid sequence of MCa_F in single letter code. The positions of half-cystine residues are highlighted in red. Cys residues are numbered and basic amino acids are highlighted in blue. Secondary structures (β strands) are indicated by arrows. The grey box is the sequence of homology of MCa with the dihydropyridine-sensitive $Ca_v1.1$ channel. (B) Amino acid sequences of unfolded MCa analogues in single letter code. Cys residues are replaced by isosteric 2-aminobutyric acid residues (Abu, in red) to form MCa_{UF1-33}. An additional N-terminal (C-MCa_{UF1-33}) or C-terminal (MCa_{UF1-33}-C) Cys residue was added in two novel analogues competent for cargo grafting (shown in grey). (C) Confocal microscopy images illustrating cell penetration of Cy5-C-MCa_{UF1-33} and MCa_{UF1-33}-C-Cy5 (green labeling). Plasma membranes are labeled with concanavalin-A-rhodamine (in red). CHO cells were incubated 2 hrs with 1 µM peptide concentration. (D) Comparison of cell penetration efficacy between Cy5-C-MCa_{UF1-33} and MCa_{UF1-33}-C-Cy5 as determined by FACS. CHO cells were incubated 2 hrs with 3 µM peptide, washed, and treated 5 min by 1 mg/ml trypsin before quantification of intracellular fluorescence.

Fig. 2. Primary structure of truncated MCa_{UF} analogues and comparison of cell penetration efficacies. (A) Primary structures of truncated MCa_{UF}-C analogues and determination of their net positive charge and percentage of basic amino acid residues within the sequence. A total of 12 truncated MCa_{UF}-C analogues were produced (three with truncations in C-terminus, seven in N-terminus, and two in both N- and C-termini). Positively charged residues are in blue (His residues were not counted), whereas Abu residues that replace Cys residues are in red. (B) Comparative cell penetration efficacy of all MCa_{UF}-C-Cy5 truncated analogues that possess a net positive charge ≥ +5. Code colors: red (net charge +8), blue (+7), pink (+6) and green (+5). The non-truncated MCa_{UF1-33}-C-Cy5 analogue is shown as reference (black line) for the efficacy of cell penetration of all analogues. Experimental conditions: CHO cell incubation with 1 µM of each analogue for 2 hrs and fluorescence quantification by FACS. (C) Same as (B) but for truncated MCa_{UF}-C-Cy5 analogues with positive net charge ≤ +2.

Fig. 3. All truncated MCa_{UF}-C-Cy5 vector/cargo complexes have resembling intracellular distributions. (A) Intracellular distribution of N-terminal truncated MCa_{UF} analogues. (B) Intracellular distribution of C-terminal truncated MCa_{UF} analogues. (C) Intracellular distribution of N- and C-terminal truncated MCa_{UF} analogues. CHO cells were incubated 2 hrs with 3 µM of MCa_{UF}-C-Cy5 vector/cargo complexes, before extensive washing, membrane labeling with rhodamine-conjugated concanavalin A, and live cell confocal microscopy imaging. Cy5 is in blue, and rhodamine in red. White arrows illustrate a tendency for a preferential apical localization of the Cy5 dye. Yellow arrows illustrate the tendency for a sub-plasma membrane labeling of the Cy5 dye.

Fig. 4. Membrane staining is diffuse whereas intracellular staining is punctuated. (A) Lower magnification image of CHO cells stained with 3 µM $MCa_{UF14-25}$-C-Cy5 that illustrates a predominant sub-plasma membrane rim-like distribution. (B) Diffuse membrane staining of CHO cells by $MCa_{UF22-33}$-C-Cy5. White arrows indicate domains of the plasma membrane where the diffuse staining of the peptide/cargo complex is the most evident. (C) Extent of colocalization of the Cy5-labeled peptides with the rhodamine-labeled plasma membrane. NS, non significant; * ≤ 0.1; ** ≤ 0.05; and *** ≤ 0.001.

Fig. 5. Amiloride sensitivity of truncated MCa_{UF} peptide cell entry. (A) Representative FACS analyses of the effect of 5 mM amiloride on MCa_{UF1-33}-C-Cy5 (upper left panel), MCa_{UF1-15}-C-Cy5 (upper right panel), $MCa_{UF20-33}$-C-Cy5 (lower left panel) and $MCa_{UF18-33}$-C-Cy5 (lower right panel) entries. Numbers in red represent average decrease or increase in peptide entry upon amiloride treatment. Cells were treated 2 hrs with 3 µM peptide concentration with or without 5 mM amiloride. (B) Average effect of amiloride on mean cell entry of the truncated peptides. Positive values reflect increase in cell entries, whereas negative values indicate reduction in cell penetration.

Fig. 6. Dose-dependent cell penetration of truncated MCaUF peptides. (A) Representative example of the dose-dependent cell penetration of MCa_{UF8-33}-C-Cy5 in CHO cells as analyzed by FACS. The peptide was incubated 2 hrs with the cells before analyses. There was no saturation of cell entry for a concentration up to 33 µM. (B) Dose-dependent cell penetration of N-terminal truncated MCa_{UF} peptides compared to MCa_{UF1-33}-C-Cy5 (open circle, dotted line). (C) Dose-dependent cell penetration of C-terminal truncated MCa_{UF} peptides. (D) Dose-dependent cell penetration of N- and C-terminal truncated MCa_{UF} peptides. Note the increase in scale for the penetration of these two peptides.

Fig. 7. Lack of pharmacological effects of the truncated peptides and reduced cell toxicity. (A) Effect of MCa_F, MCa_{UF1-33} and truncated MCa_{UF} peptides on [^{3}H]-ryanodine binding. Data were expressed as fold increase in binding induced by the peptides. (B) Effect of 1 and 10 µM MCa_{UF1-33} and truncated MCa_{UF} peptides on CHO cell viability. Peptides were incubated 24 hrs with the cells *in vitro*.

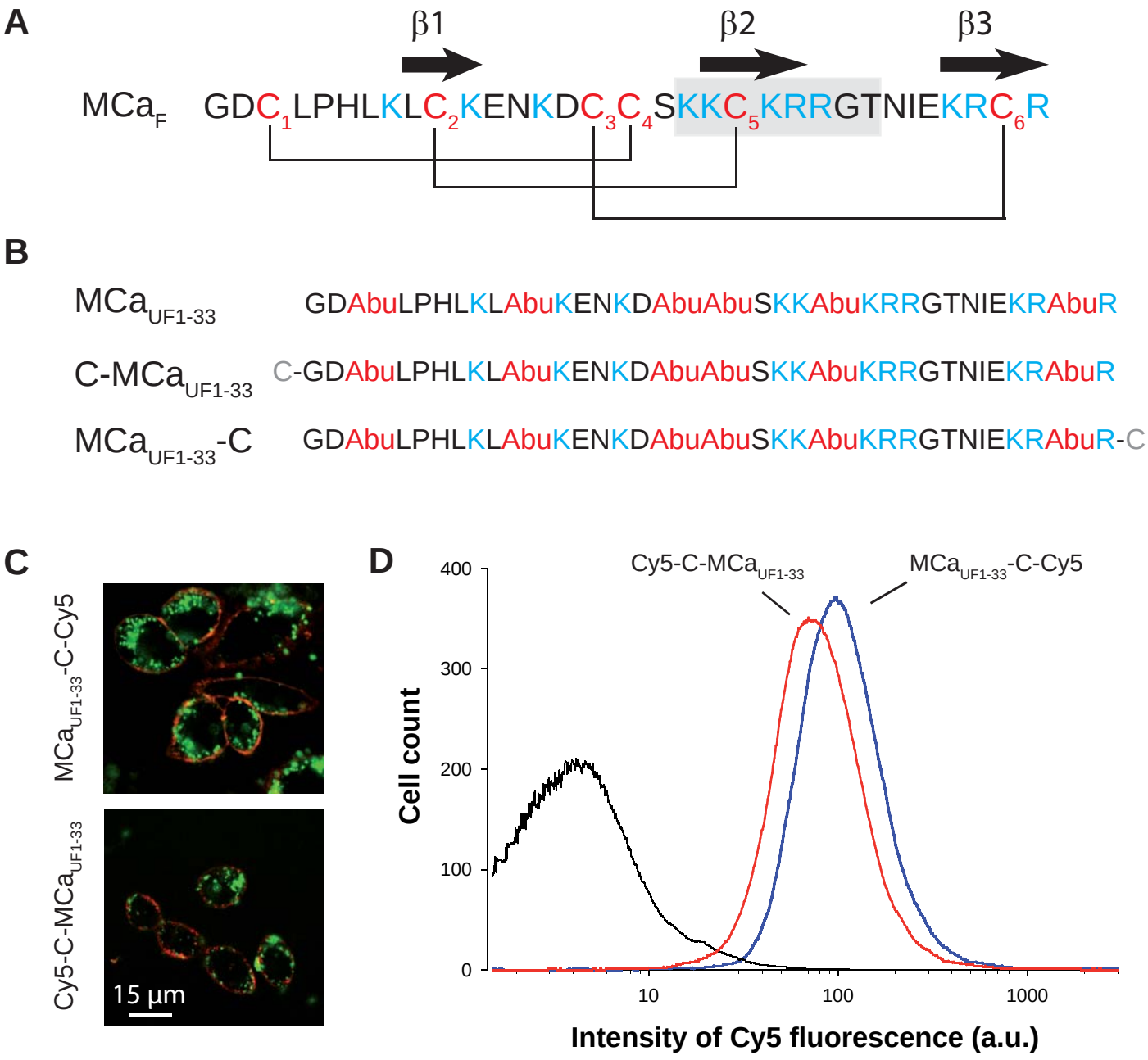
A
β1
β2
β3
MCa$_F$ GDC$_1$LPHLKLC$_2$KENKDC$_3$C$_4$SKKC$_5$KRRGTNIEKRC$_6$R
B
MCa$_{UF1-33}$ GDAbuLPHLKLAbuKENKDAbuAbuSKKAbuKRRGTNIEKRAbuR
C-MCa$_{UF1-33}$ C-GDAbuLPHLKLAbuKENKDAbuAbuSKKAbuKRRGTNIEKRAbuR
MCa$_{UF1-33}$-C GDAbuLPHLKLAbuKENKDAbuAbuSKKAbuKRRGTNIEKRAbuR-C
C
MCa$_{UF1-33}$-C-Cy5
Cy5-C-MCa$_{UF1-33}$
15 µm
D
Cy5-C-MCa$_{UF1-33}$
MCa$_{UF1-33}$-C-Cy5
Cell count
400
300
200
100
0
10
100
1000
Intensity of Cy5 fluorescence (a.u.)

Figure 1

A

		Net charge (NC)	%
MCa_{UF1-33}-C	GDAbuLPHLKLAbuKENKDAbuAbuSKKAbuKRRGTNIEKRAbuR-C	+7	33
MCa_{UF1-20}-C	GDAbuLPHLKLAbuKENKDAbuAbuSKK-C	+2	25
MCa_{UF1-15}-C	GDAbuLPHLKLAbuKENKD-C	0	20
MCa_{UF1-9}-C	GDAbuLPHLKL-C	0	11
MCa_{UF8-33}-C	KLAbuKENKDAbuAbuSKKAbuKRRGTNIEKRAbuR-C	+8	42
$MCa_{UF11-33}$-C	KENKDAbuAbuSKKAbuKRRGTNIEKRAbuR-C	+7	43
$MCa_{UF14-33}$-C	KDAbuAbuSKKAbuKRRGTNIEKRAbuR-C	+7	45
$MCa_{UF18-33}$-C	SKKAbuKRRGTNIEKRAbuR-C	+7	50
$MCa_{UF20-33}$-C	KAbuKRRGTNIEKRAbuR-C	+6	50
$MCa_{UF22-33}$-C	KRRGTNIEKRAbuR-C	+5	50
$MCa_{UF25-33}$-C	GTNIEKRAbuR-C	+2	33
MCa_{UF6-25}-C	HLKLAbuKENKDAbuAbuSKKAbuKRRG-C	+6	40
$MCa_{UF14-25}$-C	KDAbuAbuSKKAbuKRRG-C	+5	50

B

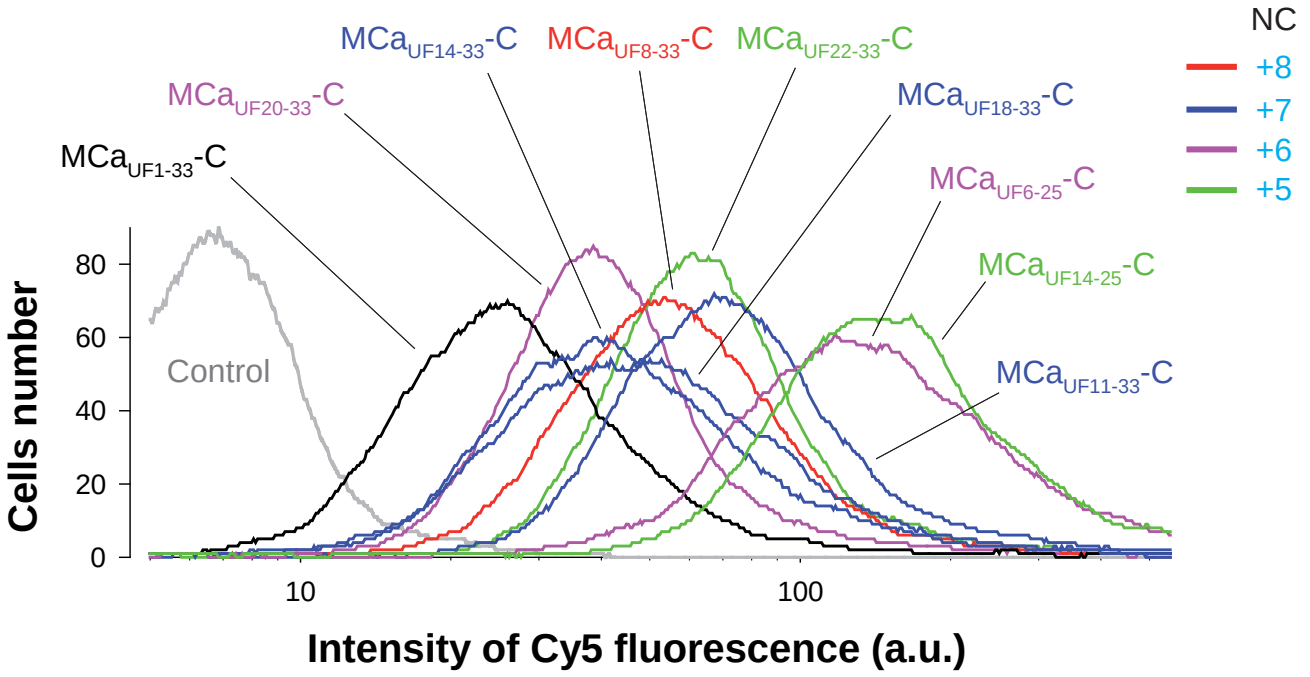

C

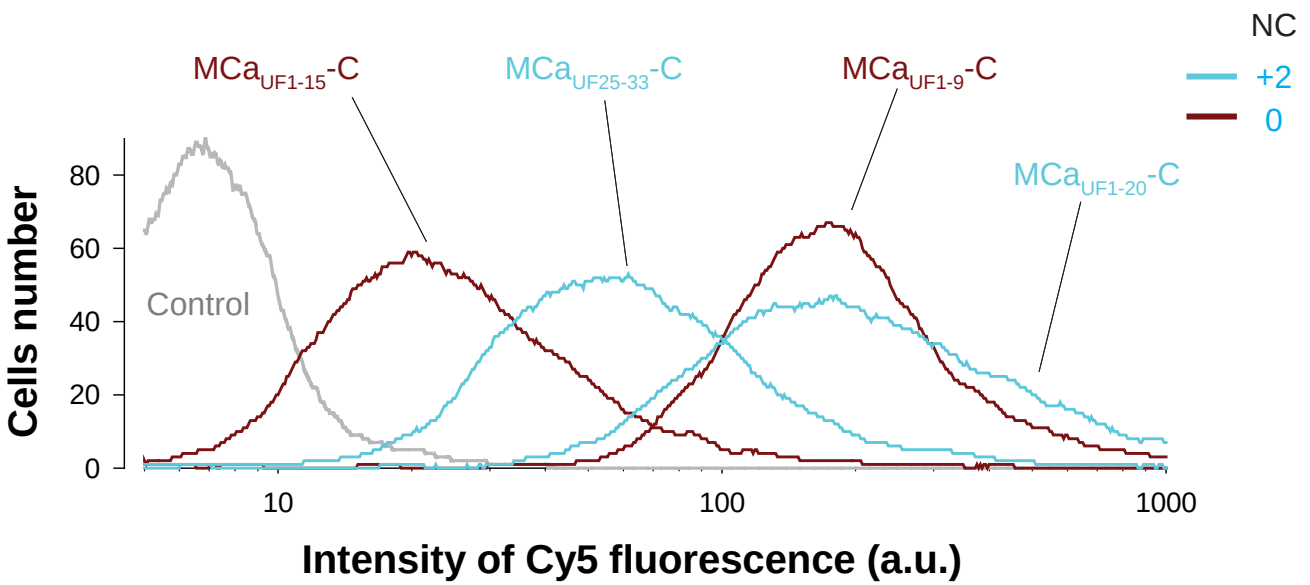

Figure 2

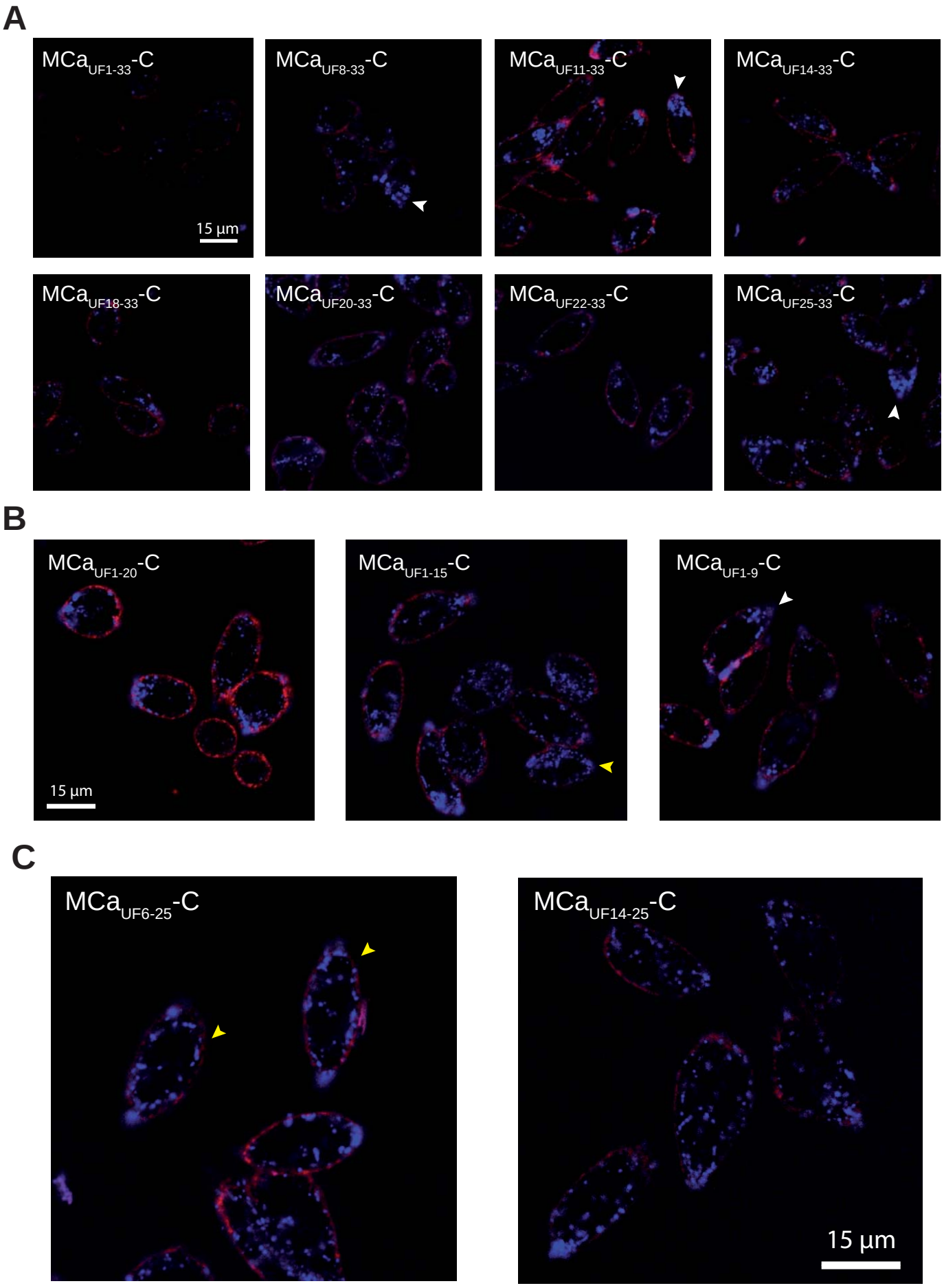
A
MCa$_{UF1-33}$-C
15 µm
MCa$_{UF8-33}$-C
MCa$_{UF11-33}$-C
MCa$_{UF14-33}$-C
MCa$_{UF18-33}$-C
MCa$_{UF20-33}$-C
MCa$_{UF22-33}$-C
MCa$_{UF25-33}$-C
B
MCa$_{UF1-20}$-C
15 µm
MCa$_{UF1-15}$-C
MCa$_{UF1-9}$-C
C
MCa$_{UF6-25}$-C
MCa$_{UF14-25}$-C
15 µm

Figure 3

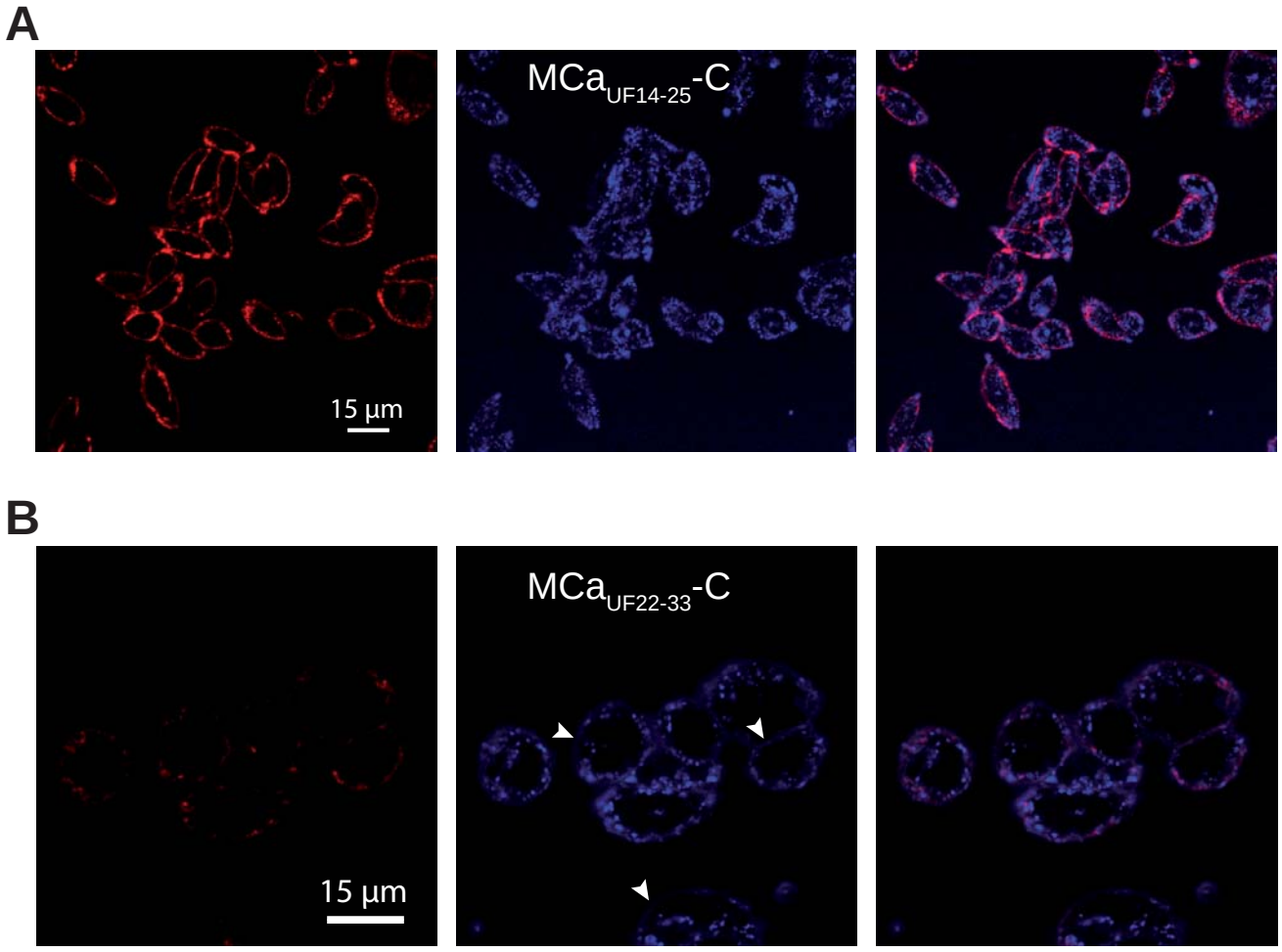
A
MCa$_{UF14-25}$-C
15 µm
B
MCa$_{UF22-33}$-C
15 µm
C
Colocalisation with plasma membrane (% pixels)
0
5
10
15
20
25
30
NS
**
**
*
NS
NS
NS
***
NS
**
NS
NS
MCa$_{UF1-33}$
MCa$_{UF8-33}$
MCa$_{UF11-33}$
MCa$_{UF14-33}$
MCa$_{UF18-33}$
MCa$_{UF20-33}$
MCa$_{UF22-33}$
MCa$_{UF25-33}$
MCa$_{UF1-20}$
MCa$_{UF1-15}$
MCa$_{UF1-9}$
MCa$_{UF14-25}$
MCa$_{UF6-25}$

Figure 5

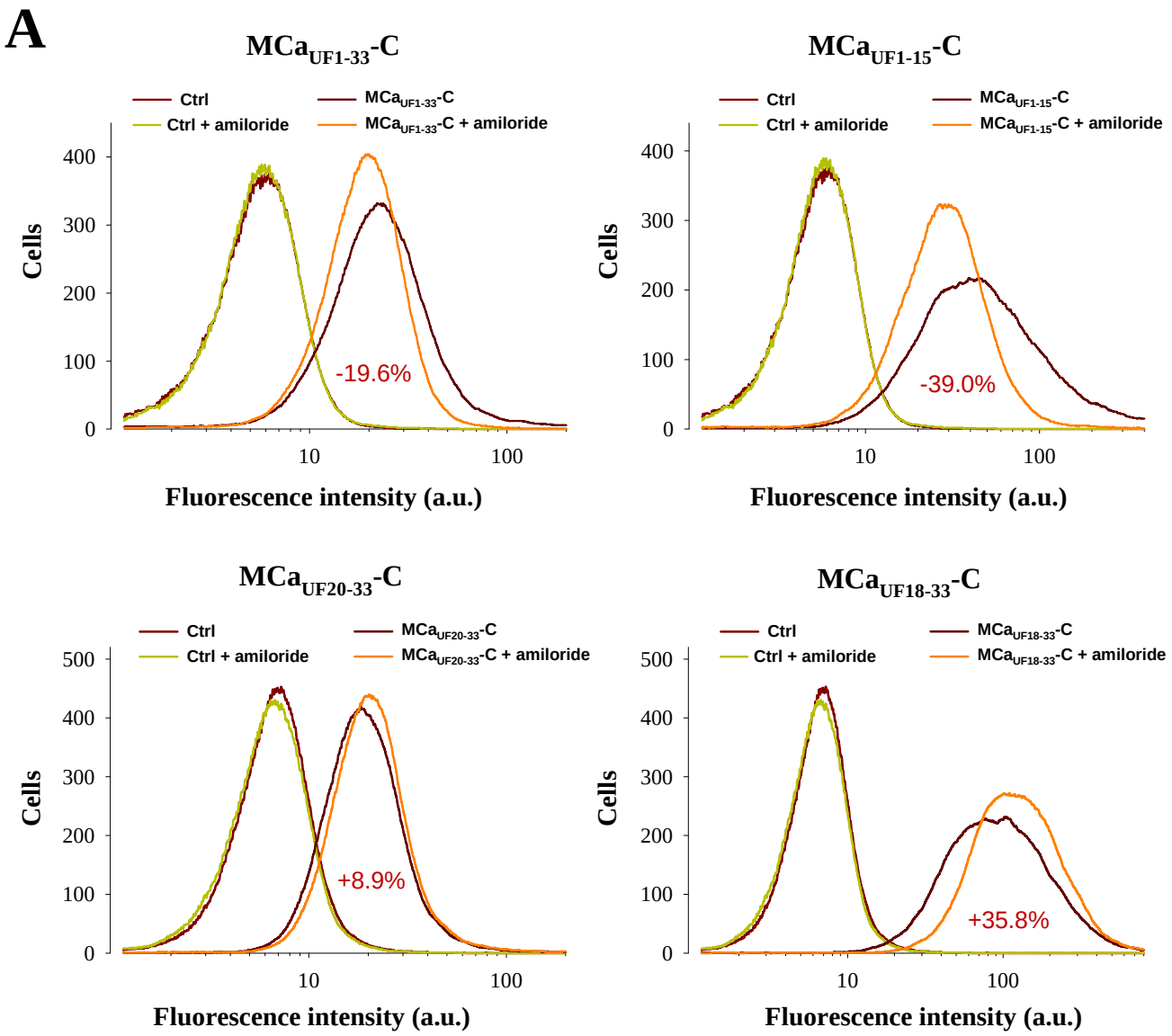
A
MCa$_{UF1-33}$-C
Ctrl
Ctrl + amiloride
MCa$_{UF1-33}$-C
MCa$_{UF1-33}$-C + amiloride
Cells
-19.6%
Fluorescence intensity (a.u.)
MCa$_{UF1-15}$-C
Ctrl
Ctrl + amiloride
MCa$_{UF1-15}$-C
MCa$_{UF1-15}$-C + amiloride
Cells
-39.0%
Fluorescence intensity (a.u.)
MCa$_{UF20-33}$-C
Ctrl
Ctrl + amiloride
MCa$_{UF20-33}$-C
MCa$_{UF20-33}$-C + amiloride
Cells
+8.9%
Fluorescence intensity (a.u.)
MCa$_{UF18-33}$-C
Ctrl
Ctrl + amiloride
MCa$_{UF18-33}$-C
MCa$_{UF18-33}$-C + amiloride
Cells
+35.8%
Fluorescence intensity (a.u.)

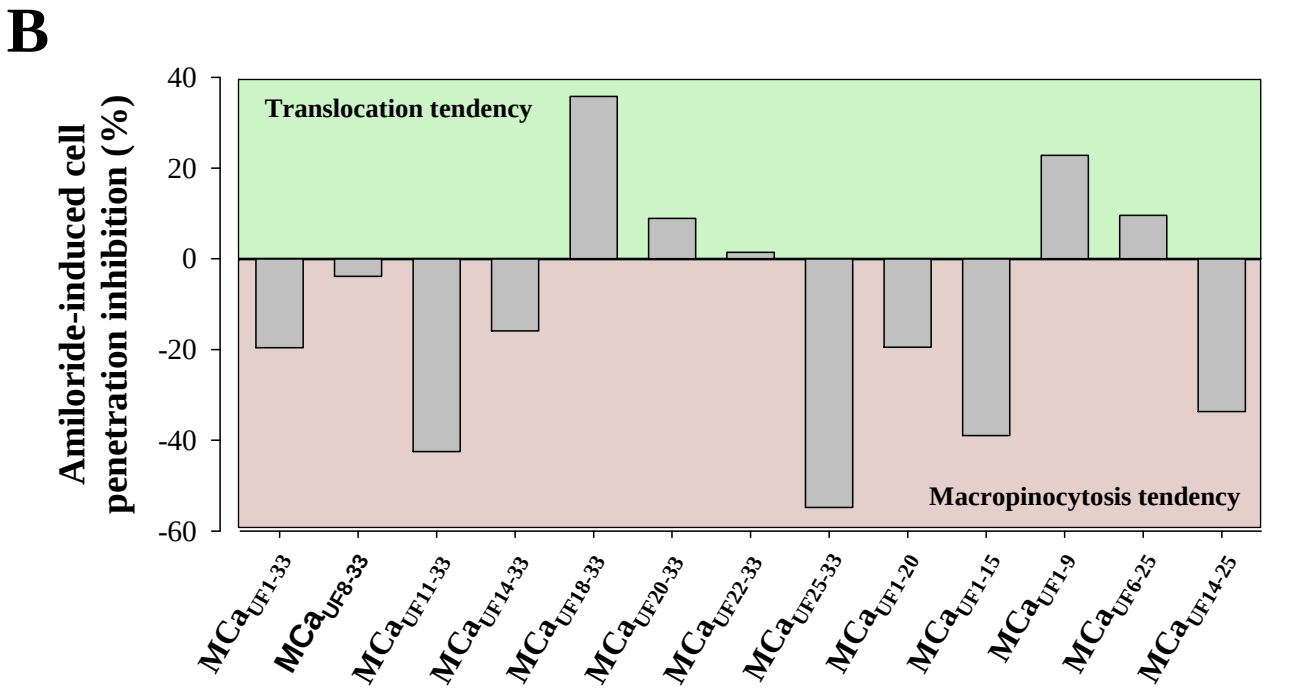
B
Amiloride-induced cell penetration inhibition (%)
Translocation tendency
Macropinocytosis tendency
MCa$_{UF1-33}$
MCa$_{UF8-33}$
MCa$_{UF11-33}$
MCa$_{UF14-33}$
MCa$_{UF18-33}$
MCa$_{UF20-33}$
MCa$_{UF22-33}$
MCa$_{UF25-33}$
MCa$_{UF1-20}$
MCa$_{UF1-15}$
MCa$_{UF1-9}$
MCa$_{UF6-25}$
MCa$_{UF14-25}$

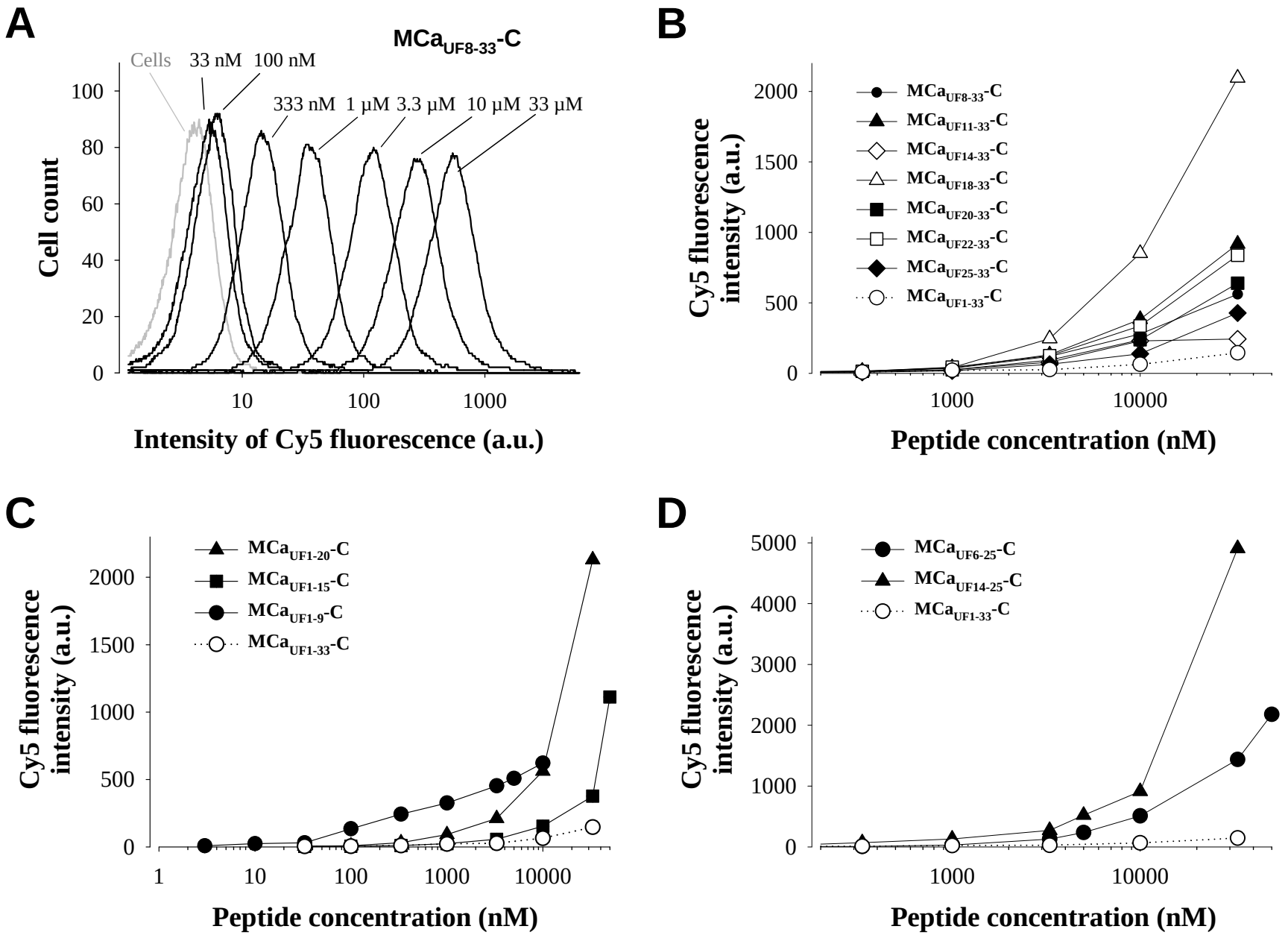
A
MCa$_{UF8-33}$-C
Cells
33 nM
100 nM
333 nM
1 µM
3.3 µM
10 µM
33 µM
Cell count
Intensity of Cy5 fluorescence (a.u.)
B
MCa$_{UF8-33}$-C
MCa$_{UF11-33}$-C
MCa$_{UF14-33}$-C
MCa$_{UF18-33}$-C
MCa$_{UF20-33}$-C
MCa$_{UF22-33}$-C
MCa$_{UF25-33}$-C
MCa$_{UF1-33}$-C
Cy5 fluorescence intensity (a.u.)
Peptide concentration (nM)
C
MCa$_{UF1-20}$-C
MCa$_{UF1-15}$-C
MCa$_{UF1-9}$-C
MCa$_{UF1-33}$-C
Cy5 fluorescence intensity (a.u.)
Peptide concentration (nM)
D
MCa$_{UF6-25}$-C
MCa$_{UF14-25}$-C
MCa$_{UF1-33}$-C
Cy5 fluorescence intensity (a.u.)
Peptide concentration (nM)

Figure 6

Figure 7

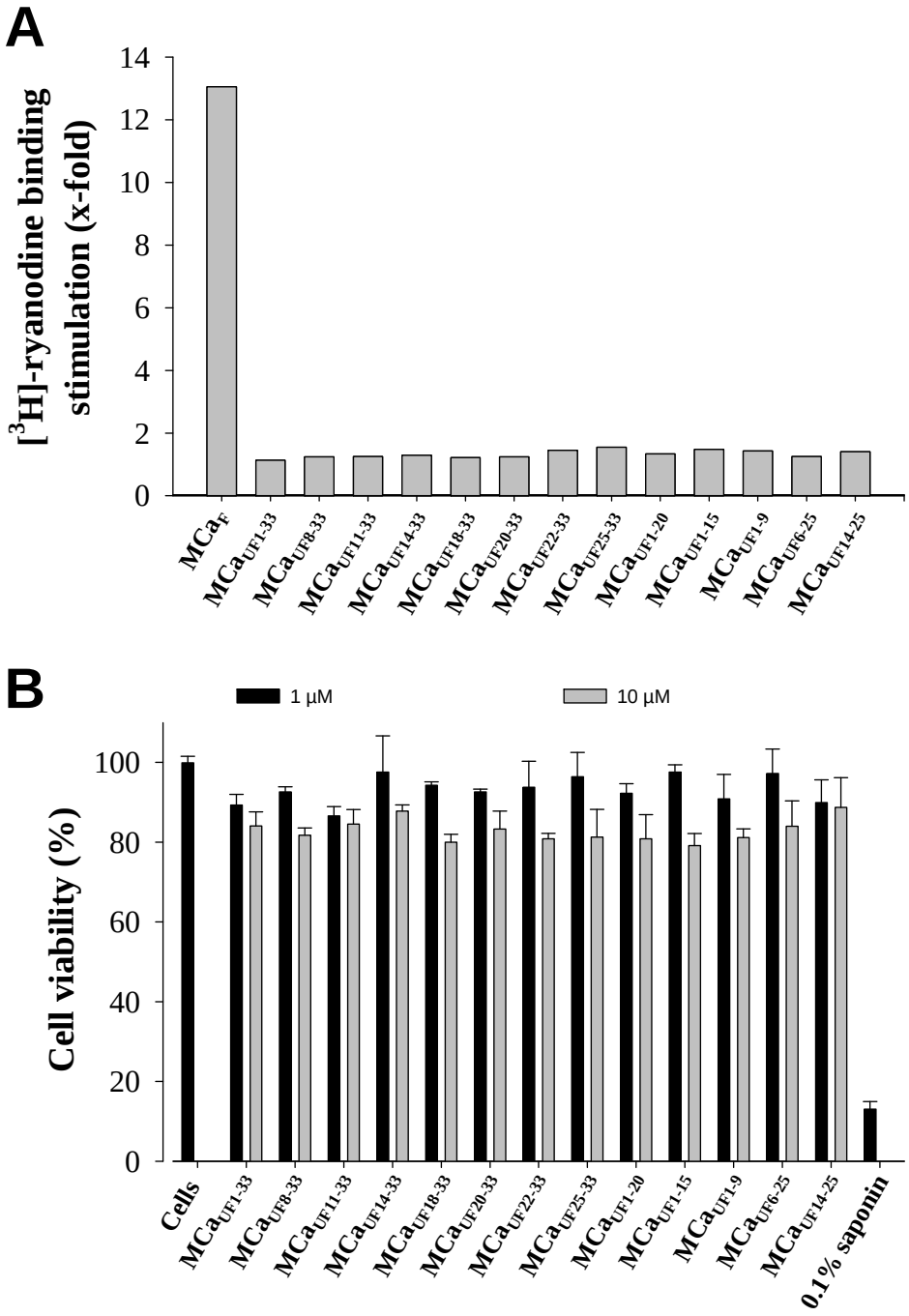
A
[3H]-ryanodine binding stimulation (x-fold)
14
12
10
8
6
4
2
0
MCaF
MCaUF1-33
MCaUF8-33
MCaUF11-33
MCaUF14-33
MCaUF18-33
MCaUF20-33
MCaUF22-33
MCaUF25-33
MCaUF1-20
MCaUF1-15
MCaUF1-9
MCaUF6-25
MCaUF14-25
B
1 µM
10 µM
Cell viability (%)
100
80
60
40
20
0
Cells
MCaUF1-33
MCaUF8-33
MCaUF11-33
MCaUF14-33
MCaUF18-33
MCaUF20-33
MCaUF22-33
MCaUF25-33
MCaUF1-20
MCaUF1-15
MCaUF1-9
MCaUF6-25
MCaUF14-25
0.1% saponin